

Delineation of the First Human Mendelian Disorder of the DNA Demethylation Machinery: *TET3* Deficiency

David B. Beck,¹ Ana Petracovici,^{2,3,4} Chongsheng He,^{3,4,5} Hannah W. Moore,⁶ Raymond J. Louie,⁶ Muhammad Ansar,⁷ Sofia Douzgu,^{8,9} Sivagamy Sithambaram,⁹ Trudie Cottrell,⁹ Regie Lyn P. Santos-Cortez,¹⁰ Eloise J. Prijoles,⁶ Renee Bend,⁶ Boris Keren,¹¹ Cyril Mignot,^{11,12} Marie-Christine Nougues,¹³ Katrin Öunap,^{14,15} Tiia Reimand,^{14,15,16} Sander Pajusalu,^{14,15,17} Muhammad Zahid,⁷ Muhammad Arif Nadeem Saqib,¹⁸ Julien Buratti,¹¹ Eleanor G Seaby,^{19,20} Kirsty McWalter,²¹ Aida Telegrafi,²¹ Dustin Baldrige,²² Marwan Shinawi,²² Suzanne M. Leal,²³ G. Bradley Schaefer,²⁴ Roger E. Stevenson,⁶ Siddharth Banka,^{8,9} Roberto Bonasio,^{3,4} and Jill A. Fahrner^{25*}

¹National Human Genome Research Institute, National Institutes of Health, Bethesda, MD, 20892, USA

²Graduate Group in Genetics and Epigenetics, University of Pennsylvania Perelman School of Medicine, Philadelphia, PA, 19104, USA

³Department of Cell and Developmental Biology, University of Pennsylvania Perelman School of Medicine, Philadelphia, PA, 19104, USA

⁴Epigenetics Institute, University of Pennsylvania Perelman School of Medicine, Philadelphia, PA, 19104, USA

⁵Current address: Hunan Key Laboratory of Plant Functional Genomics and Developmental Regulation, Hunan University, Changsha, 410082 Hunan, P.R. China

⁶Greenwood Genetic Center, Greenwood, SC, 29646, USA

⁷Department of Biochemistry, Faculty of Biological Sciences, Quaid-I-Azam University, 45320, Islamabad, Pakistan

⁸Division of Evolution & Genomic Sciences, School of Biological Sciences, Faculty of Biology, Medicine and Health, University of Manchester, Manchester, M13 9PL, UK

⁹Manchester Centre for Genomic Medicine, St Mary's Hospital, Manchester University NHS Foundation Trust, Health Innovation Manchester, Manchester, M13 9WL, UK.

¹⁰Department of Otolaryngology, University of Colorado School of Medicine, Aurora, CO, 80045, USA

¹¹Assistance Publique-Hôpitaux de Paris, Groupe Hospitalier Pitié-Salpêtrière, Département de

Génétique, Paris, 75013, France

¹²Centre de Référence Déficiences Intellectuelles de Causes Rares, Paris, France

¹³ Assistance Publique-Hôpitaux de Paris, Armand Trousseau Hospital, Department of Neuropediatrics, Paris, 75012, France

¹⁴Department of Clinical Genetics, United Laboratories, Tartu University Hospital, Tartu, 50406, Estonia

¹⁵Department of Clinical Genetics, Institute of Clinical Medicine, University of Tartu, Tartu, Estonia

¹⁶Chair of Human Genetics, Institute of Biomedicine and Translational Medicine, University of Tartu, Tartu, Estonia

¹⁷Yale University School of Medicine, Department of Genetics, New Haven, CT, USA

¹⁸Pakistan Health Research Council, 45320, Islamabad, Pakistan

¹⁹Program in Medical and Population Genetics, Broad Institute of MIT and Harvard, Cambridge, Massachusetts 02142, USA

²⁰Analytic and Translational Genetics Unit, Massachusetts General Hospital, Boston, Massachusetts 02114, USA

²¹GeneDx, Gaithersburg, Maryland, 20877, USA

²²Department of Pediatrics, Division of Genetics and Genomic Medicine, Washington University School of Medicine, St. Louis, MO, 63110, USA

²³Center for Statistical Genetics, Gertrude H. Sergievsky Center, Taub Institute for Alzheimer's Disease and the Aging Brain, Department of Neurology, Columbia University Medical Center, 630 W 168th St, New York, NY 10032.

²⁴University of Arkansas for Medical Sciences, Lowell, AK, 72745, USA

²⁵Department of Pediatrics, McKusick-Nathans Institute of Genetic Medicine, Johns Hopkins University, Baltimore, MD, 21205, USA

*Correspondance: jfahrne1@jhmi.edu

ABSTRACT

Germline pathogenic variants in chromatin-modifying enzymes are a common cause of pediatric developmental disorders. These enzymes catalyze reactions that regulate epigenetic inheritance via histone post-translational modifications and DNA methylation. Cytosine methylation of DNA (5mC) is the quintessential epigenetic mark, yet no human Mendelian disorder of DNA demethylation has been delineated. Here, we describe in detail the first Mendelian disorder caused by disruption of DNA demethylation. *TET3* is a methylcytosine dioxygenase that initiates DNA demethylation during early zygote formation, embryogenesis, and neuronal differentiation and is intolerant to haploinsufficiency in mice and humans. Here we identify and characterize 11 cases of human *TET3* deficiency in 8 families with the common phenotypic features of intellectual disability/global developmental delay, hypotonia, autistic traits, movement disorders, growth abnormalities, and facial dysmorphism. Mono-allelic frameshift and nonsense variants in *TET3* occur throughout the coding region. Mono-allelic and bi-allelic missense variants localize to conserved residues with all but one occurring within the catalytic domain and most displaying hypomorphic function in a catalytic activity assay. *TET3* deficiency shows substantial phenotypic overlap with other Mendelian disorders of the epigenetic machinery, including intellectual disability and growth abnormalities, underscoring shared disease mechanisms.

Introduction

Post-translational modifications of histone tails and DNA methylation play essential roles in development by regulating chromatin structure and gene expression. Inherited conditions that disrupt these processes – chromatin-modifying enzyme disorders or Mendelian disorders of the epigenetic machinery - account for a substantial percentage of neurodevelopmental and growth abnormalities in children ^{1;2}. Most known disorders in this class are caused by pathogenic variants in histone-modifying enzymes and chromatin remodelers. Far fewer have been linked to deficiencies in the DNA methylation machinery³⁻⁵. The latter include disorders caused by defects in DNA methylation “writers,” or DNA methyltransferases (DNMTs), such as immunodeficiency-centromeric instability-facial anomalies syndrome-1 (ICF syndrome) due to bi-allelic variants in *DNMT3B* (MIM: 242860), and Tatton-Brown-Rahman syndrome due to mono-allelic variants in *DNMT3A* (MIM: 615879), or by defects in reader proteins that bind to DNA methylation, such as Rett syndrome, which is caused by variants in *MECP2* (MIM: 312750) ³⁻⁵. No Mendelian disorder has been linked to the multi-step and tightly regulated process that removes DNA methylation.

The roles of DNMTs and proteins like *MECP2* in “writing” and “reading” methyl marks on DNA have been known for decades, whereas the existence of enzymes that can actively reverse or “erase” DNA methylation was discovered more recently ^{6;7}. The ten-eleven translocase (TET) family of enzymes consists of three methylcytosine dioxygenases (TET1, TET2, and TET3) that initiate DNA demethylation through a series of sequential oxidation reactions converting 5-methyl cytosine (5mC) first to 5-hydroxymethylcytosine (5hmC) and then to 5-formylcytosine (5fC) and 5-carboxylcytosine (5caC), which are removed either passively by replication-dependent dilution or actively by thymidine DNA glycosylase ⁸. The process ultimately results in loss of the methylated base and replacement with an unmethylated cytosine ^{6;7;9;10}, effectively leading to DNA demethylation.

In addition to being an intermediate in the active removal of 5mC, 5hmC is suggested to have an independent role in gene regulation, though the exact nature remains unclear. Notably, 5hmC levels differ globally based on cell lineage and are particularly enriched in mammalian brains ^{8;11}. 5fC and 5caC are less well understood and may have unique functions as well⁸. *Tet3* is highly expressed in oocytes, zygotes, and neurons, and ablation of *Tet3* in mice leads to embryonic lethality ⁸. TET3 plays an important role in rapidly demethylating the paternal genome after fertilization, producing genome-wide increases in the oxidized 5mC intermediates 5hmC, 5fC, and 5caC ¹²⁻¹⁶. Importantly, *Tet3* haploinsufficiency causes neonatal sublethality or sub-Mendelian ratios in mice ¹⁷. Furthermore, inhibition or depletion of *Tet3* in mouse differentiated

neurons can impact synaptic function¹⁸⁻²⁰. In humans, *TET3* is highly intolerant to loss-of-function alleles in control databases²¹, and homozygous missense variants in *TET3* were recently implicated as a possible cause for autosomal recessive intellectual disability in a single consanguineous family (further described here as family 3)²². Together, these findings illustrate the important role of *TET3* in early embryonic development and neuronal function.

Here, we provide the first detailed description of a cohort of individuals with a Mendelian disorder due to disruption of the DNA demethylation machinery, namely the *TET3* enzyme. Whereas inheritance patterns vary and include both autosomal dominant and autosomal recessive forms, all affected individuals have in common a deficiency in *TET3* function. This is either due to one or more missense variants within the highly conserved catalytic domain, most of which have been functionally validated to possess decreased *TET3* activity, or to a single frameshift or nonsense variant. The phenotype is remarkably similar between affected individuals and is consistent with the broader group of Mendelian disorders of the epigenetic machinery, which often show global developmental delay/intellectual disability and other neurological manifestations, growth abnormalities, and characteristic craniofacial features^{1 23 24}.

Results

Individual 1 presented with developmental delay, generalized overgrowth including macrocephaly, and some facial features reminiscent of Sotos syndrome (**Table 1**). Targeted testing for Sotos syndrome (MIM: 117550; *NSD1*) and the related Malan syndrome (MIM: 614753; *NFIX*), as well as methylation testing for Beckwith Wiedemann syndrome (MIM# 130650) and array comparative genomic hybridization (CGH), were negative. We performed research-based trio exome sequencing and identified bi-allelic rare variants in *TET3* (NM_001287491.1 c.2254C>T; p.Arg752Cys and c.3265C>A; p.Val1089Met). Through collaborations with other institutions and Genematcher²⁵ we subsequently identified an additional 10 affected individuals in 7 unrelated families with overlapping phenotypes and rare variants in *TET3* predicted to negatively impact catalytic function (**Table 1; Figure 1**).

To delineate the phenotypic spectrum associated with variants in *TET3* we collected detailed clinical information on all affected individuals, who ranged in age from 11 months to 43 years at the time of assessment (**Table 1**). We observed striking phenotypic overlap among affected individuals (**Table 1**). All had global developmental delay and/or intellectual disability, and the vast majority had hypotonia and/or joint hypermobility (9/11). Other commonly observed findings were autistic features including difficulty with social interactions (6/11), growth

abnormalities (8/11), movement disorders (5/11), and overlapping common facial characteristics (**Figure 1**). The developmental delay/intellectual disability ranged from mild to severe and included gross motor delay with or without speech delay in almost all cases (**Table 1**). Seizures and/or EEG abnormalities occurred in 4/11 individuals; other movement disorders were also noted and included tics, dystonia, extensor posturing, and myoclonic jerks (**Table 1**). Brain MRI demonstrated non-specific abnormalities in two individuals, including periventricular white matter changes and increased extra-axial spaces including ventriculomegaly (**Table 1**). Postnatal growth abnormalities were identified in 7/11 affected individuals, most often involving head size, with three individuals (1, 4, and 5) having true macrocephaly (OFC $\geq +2$ SD above the mean), one (6) having borderline/relative macrocephaly, and two (3-I and 3-III) having microcephaly (**Table 1**). In individual 1, macrocephaly is accompanied by tall stature (height $\geq +2$ SD above the mean), and in individual 3-I, microcephaly is accompanied by short stature (height ≤ -2 SD below the mean; **Table 1**). Three individuals (3-I, 3-III, and 6) were born small for gestational age, suggesting a potential effect on prenatal growth; however, two of these were siblings from the same consanguineous family, and we cannot rule out other genetic causes, maternal factors, exposures, or poor prenatal care without additional information. The other individual born small for gestational age (individual 6) continued to exhibit poor weight gain but developed borderline macrocephaly by 18 months of age (**Table 1**). Distinctive craniofacial features common to these patients include tall and/or broad forehead (6/11) and long face (5/11; **Table 1**). Less commonly noted were brachycephaly (4/11), short nose and long philtrum particularly in younger individuals (4/11), hypotonic facies with open mouth appearance (4/11), protruding ears (4/11), and highly arched palate (3/11; **Table 1**). A few had feeding difficulties (3/11), and eye findings including nystagmus (2/11; **Table 1**).

Five cases in three distinct families had bi-allelic variants, consistent with autosomal recessive inheritance (**Table 1**; **Figure 1**). Two of these individuals were compound heterozygotes, whereas the other three were siblings from a consanguineous family homozygous for the same variant (**Table 1**; **Figure 1**)²². In all three of the autosomal recessive families, at least one parent appeared mildly affected. Both parents of individual 2 had mild learning difficulties requiring individualized educational plans (IEPs) in school; in addition, the father had attention deficit hyperactivity disorder (ADHD), and the mother had a history of seizures requiring medication in childhood. The mother of individuals 3-I, 3-II, and 3-III has severe anxiety, problems with short-term memory, and borderline psychosis, whereas the parental phenotypes in family 1 appear milder with the father and unaffected sister having specific and similar mild childhood learning disabilities, and the mother having occasional depression, significant anxiety, and

possible ADHD, the latter two also confirmed in her affected daughter. All parents were able to live independently and/or hold jobs.

In terms of specific variants, all five autosomal recessive cases from three distinct lineages (**Figure 1; Table 1**) harbor either rare or novel missense changes at conserved residues within or adjacent to the catalytic domain of TET3 (**Figure 2A-B**), which consists of a dioxygenase domain separated by a spacer and a cystine-rich domain (**Figure 2A**). Specifically, individual 1 has a paternally inherited c.2254C>T (p.Arg752Cys) variant just upstream of the catalytic domain and a maternally inherited c.3265G>A (p.Val1089Met) variant within the dioxygenase domain; individual 2 has a paternally inherited c.3215T>G (p.Phe1072Thr) variant and a maternally inherited c.3226G>A (p.Ala1076Thr) variant, both of which are in the dioxygenase domain (**Figure 2A**). Individuals 3-I, 3-II, and 3-III are siblings from a consanguineous family and share the c.2722G>T (p.Val908Leu) homozygous variant²² within the cystine-rich domain (**Figure 2A**). We mapped these potential variants in *TET3* to the well-conserved TET2 catalytic domain crystal structure, and all but one (p.Arg752Cys) could be visualized (**Figure 2C**). Val1089Met and Phe1072Thr are in close proximity to residue Asn1387 of TET2, which forms a hydrogen bond with the cytosine base of 5hmC to stabilize binding. Ala1076 is found adjacent to Thr1393 of TET2 which participates in hydrogen bonding with the N4 exocyclic amino group of cytosine²⁶.

In addition, we identified six individuals in five families with rare mono-allelic variants in *TET3* suggestive of autosomal dominant inheritance (**Table 1; Figure 1**). One was inherited, and the rest occurred *de novo*. In family 7, a similarly affected father and son both harbor the same frameshift variant c.4977_4983del (p.His1660ProfsTer52) in the catalytic domain (**Figure 2A**), consistent with autosomal dominant inheritance. Individual 5 has a *de novo* nonsense variant c.5083C>T (p.Gln1695Ter) also located within the dioxygenase domain, and both this and the inherited variant occur in the last exon (**Figure 2A**). Individual 8 has a *de novo* frameshift variant c.1215delA (p.Trp406GlyfsX135) upstream of the catalytic domain (**Figure 2A**), and individuals 4 and 6 harbor *de novo* missense variants, namely c.2552C>T (p.Thr851Met) and c.5030C>T (p.Pro1677Leu), with the former located in the cystine-rich domain and the latter within the dioxygenase domain (**Figure 2A**). Notably, in both autosomal recessive and autosomal dominant cases, all missense variants (except for p.Arg752Cys) are located within the catalytic domain (**Figure 2A**), and moreover, all occurred at residues highly conserved across species with many of the variants occurring at positions also conserved among human and sometimes mouse TET enzymes (**Figure 2B**).

In the first step of DNA demethylation, 5mC is converted to 5hmC by TET enzymes⁸. To analyze the effect of individual patient variants on TET3 catalytic activity, we measured 5hmC

production using a cell culture system whereby recessively inherited TET3 variants (Arg752Cys, Phe1072Thr, Ala1076Thr, Val1089Met, and Val908Leu) were overexpressed in HEK 293 cells and total 5hmC levels were measured with a dot blot assay (**Figure 3A**). We compared the activity of TET3 variants to that of a known catalytically inactive mutant (Δ cat; p.H1077Y/D1079A) and to full length wild-type TET3 (**Figure 3B-D**). All patient variants tested demonstrated a defect in converting 5mC to 5hmC, except for Arg752Cys (**Figure 3 B,D**), which is outside the catalytic domain and not conserved among TET enzymes (**Figure 2A-B**). The observed defects were consistent across biological replicates, despite fluctuations in the levels of TET3 variant expression (**Figure S1**). For quantification, the 5hmC levels from cells expressing TET3 mutants were normalized to those measured in cells transfected with the wild-type TET3 construct to obtain a relative 5hmC signal (**Figure 3D**). These results showing decreased cellular levels of 5hmC suggest that the vast majority of the missense variants identified in affected individuals have hypomorphic function. The observation that patients with nonsense and frameshift variants have phenotypes similar to patients with hypomorphic missense variants further supports the hypothesis that decreased TET3 catalytic activity leads to disease.

Discussion

TET3, like most genes encoding components of the epigenetic machinery, is highly dosage-sensitive in both model organisms and humans^{1; 17; 21}. *TET3* has a pLI score of 1 (observed/expected=0.02), suggesting near complete intolerance to loss of function variation²¹. Based on this high pLI score and its high degree of coexpression across diverse tissues, *TET3* was recently predicted bioinformatically to be a candidate epigenetic machinery disease gene²⁷. Consistent with dosage sensitivity, most Mendelian disorders of the epigenetic machinery are autosomal dominant due to haploinsufficiency. In line with these observations, we identified patients with mono-allelic missense or loss of function (nonsense and frameshift) variants in *TET3*. However, we also report individuals with overlapping phenotypes that carry bi-allelic hypomorphic missense variants, each with mildly decreased catalytic activity according to our overexpression assay. We expect that in both cases - mono-allelic loss of function mutations and bi-allelic hypomorphic mutations - there is a similar reduction in total enzymatic activity causing a conserved disease mechanism across inheritance types. Notably, nonsense and frameshift variants were only identified in the heterozygous state, suggesting that some residual TET3 activity is required for viability. Conversely, perhaps a certain threshold of TET3 activity

exists, below which developmental phenotypes result regardless of whether reduced TET3 activity is caused by missense or loss of function heterozygous alleles or biallelic hypomorphic alleles.

Within our cohort we identified patients with autosomal recessive inheritance with mildly affected carrier parents, which is consistent with a causal relationship between perturbations of TET3 activity and disease manifestations and suggests an inverse correlation between residual TET3 activity and phenotypic severity. Similar examples of complex inheritance involving both mono-allelic and bi-allelic variants in another component of the epigenetic machinery, *KDM5B*, have been reported recently^{28; 29}. An alternative hypothesis for differential modes of inheritance other than absolute activity levels could be that mono-allelic mutations have activating or dominant negative effects while bi-allelic mutations lead to loss of function; other examples of this exist in human disease^{30; 31}. We cannot rule this out here because the nonsense and frameshift variants identified in families 5 and 7, respectively, are located in the last exon and may escape non-sense mediated decay, raising the possibility of a dominant negative mutation mechanism and warranting further mechanistic studies to better correlate genotype and phenotype.

Along these lines, despite the evidence for multiple modes of inheritance, we cannot discount the possibility that individuals with *de novo* variants have additional non-coding sequence variants *in trans*, given that exome sequencing, not genome sequencing, was performed. Similarly, we have not ruled out epigenetic alterations *in trans*, such as DNA methylation. In addition, individuals can have additional variants that contribute to their phenotype as is the case for individual 8, with a paternally inherited 16p11.2 duplication and individual 2 with a maternally-inherited 16q22.1q22.2 duplication. Further studies, including genome sequencing and methylation analysis, could shed light on the molecular mechanisms involved. However, family 7 with two sequential affected generations supports autosomal dominant inheritance, particularly when considered along with the four *de novo* cases. Together, our observations strongly support two distinct modes of inheritance for *TET3* deficiency syndrome.

Another explanation for the observed monoallelic and biallelic cases is sex-specific differences. Notably, all probands with mono-allelic variants are male whereas all but one of the individuals with bi-allelic variants are female. While it remains true that most (if not all) of the carrier mothers appear to have mild manifestations, these were not sufficient to bring them to medical attention. It therefore remains possible that males are more susceptible to *TET3* deficiency and only require a single monoallelic variant to express the full phenotype whereas

females require biallelic variants. Certainly, these sex-specific findings may be due to chance given the small total number of individuals; therefore, identification of additional affected individuals and further investigation into the mechanisms associated with specific mutations is required to fully delineate the mode of pathogenesis.

TET3-deficient individuals have significant phenotypic overlap with the broader group of Mendelian disorders of the epigenetic machinery, which are characterized by global developmental delay/intellectual disability and other neurobehavioral findings, as well as growth abnormalities including growth retardation or overgrowth^{1; 23; 24}. Tatton-Brown *et al.* recently showed that variants in epigenetic machinery genes account for approximately 45% of overgrowth co-occurring with intellectual disability and that the most common disorder within the group is Sotos syndrome, resulting from variants in *NSD1*²³. Our data suggest *TET3* deficiency may fall into this group of overgrowth and intellectual disability disorders, as all individuals with *TET3* deficiency have intellectual disability/global developmental delay and a subset have overgrowth. Among patients displaying both phenotypes, most also exhibit facial features reminiscent of Sotos syndrome, including a long face and tall forehead. This phenotypic overlap is particularly intriguing in the context of known biochemical interactions between *TET3* and *NSD* proteins³². Further support comes from observations that *TET3* also binds other epigenetic factors encoded by genes responsible for overgrowth and intellectual disability disorders, such as *SETD2* responsible for Luscan-Lumisich syndrome (MIM: 616831), *HIST1H1E* responsible for Rahman syndrome (MIM: 617537), and *SUZ12*, which causes a newly described Weaver-like syndrome^{23; 32-34}. The subset of individuals with *TET3* deficiency who exhibit overgrowth (macrocephaly) in addition to intellectual disability is mostly confined to those with mono-allelic variants and autosomal dominant inheritance (individuals 4,5,6), consistent with the established inheritance pattern of overgrowth and intellectual disability disorders²³. The exception is individual 1, who has overgrowth consisting of macrocephaly and tall stature in the setting of bi-allelic variants inherited *in trans* from carrier parents, which we initially thought indicated autosomal recessive inheritance. However, her Arg752Cys variant was the only one tested that did not show decreased *TET3* activity in our enzymatic assay, suggesting the possibility that the other p.Val1089Met variant is mostly if not solely responsible for the disease phenotype. In support of this, her mother, who carries the confirmed p.Val1089Met hypomorphic variant, does exhibit potentially relevant features, including significant anxiety and possible ADHD, although she is of average height and her head circumference measurement is unavailable. Further supporting this, the father and unaffected non-carrier sister have specific and similar mild childhood learning disabilities, which are likely

unrelated to the proband's phenotype. It therefore remains possible that the phenotype of individual 1 more closely resembles that of others with autosomal dominant inheritance. Future studies of individual mutation mechanisms will shed light on disease pathogenesis.

Together our clinical observations and biochemical studies define a novel neurodevelopmental disorder due to reduction in TET3 catalytic activity. TET3 plays a key role in actively reversing DNA methylation and is the first enzyme in the DNA demethylation system shown to cause a Mendelian disorder. Individuals with TET3 deficiency display overlapping phenotypic features with other Mendelian disorders of the epigenetic machinery, namely developmental delay/intellectual disability, other neurobehavioral manifestations, and growth abnormalities. By describing in detail for the first time a deficiency in the DNA demethylation pathway, our work defines a novel biochemical category of epigenetic machinery disorders and expands our knowledge of this important group diseases. Given the central role of DNA methylation in epigenetic inheritance, this disorder provides important initial insights into the dynamic regulation of DNA methylation in humans. Further characterization of *TET3*-deficient individuals, their causative variants, and their resulting molecular perturbations will lead to a deeper understanding of the role of DNA methylation and demethylation in human development and disease.

Acknowledgements

We would like to thank all of the participating families. R.B. acknowledges support from the NIH (DP2MH107055, R01GM127408). A.P. was supported in part by an NIH training grant (T32 HD083185). J.A.F. acknowledges support from The Hartwell Foundation (Individual Biomedical Research Award) and the National Institutes of Health (K08HD086250). We thank the Baylor-Hopkins Center for Mendelian Genomics for exome sequencing and bioinformatics analysis on family 1; this work was supported by grant 5UM1HG006542 from NHGRI and NHLBI. Work on family 6 was supported by the Estonian Research Council grants PUT355, PRG471 and PUTJD827. The Broad Center for Mendelian Genomics (UM1 HG008900) is funded by the National Human Genome Research Institute with supplemental funding provided by the National Heart, Lung, and Blood Institute under the Trans-Omics for Precision Medicine (TOPMed) program and the National Eye Institute. Work on family 3 was supported by Higher Education Commission Grant No. NRPU-7099, Pakistan, to M.A. The DDD study presents independent research commissioned by the Health Innovation Challenge Fund [grant number HICF-1009-003]. This study makes use of DECIPHER (<http://decipher.sanger.ac.uk>), which is funded by the Wellcome. See Nature PMID: 25533962 or www.ddduk.org/access.html for full acknowledgement.

Conflict of Interest:

R.J.L. is a clinical laboratory director in molecular genetics at the Greenwood Genetic Center, and the Greenwood Genetic Center receives fee income from clinical laboratory testing. A.T. and K.M. are employees of GeneDx. Otherwise the authors report no conflicts of interest.

Table 1. Clinical Characteristics of Individuals harboring *TET3* variants.

Table 1

Proband	1	2	3-I ²²	3-II ²²	3-III ²²	4	5	6	7-I	7-II	8
Variant cDNA^a	c.2254C>T (Paternal); c.3265G>A (Maternal)	c.3215T>G (Paternal); c.3226G>A (Maternal)	c.2722G>T (Maternal; Paternal)	c.2722G>T (Maternal; Paternal)	c.2722G>T (Maternal; Paternal)	c.2552C>T	c.5083C>T*	c.5030C>T*	c.4977_4983del*	c.4977_4983del*	c.1215delA
Amino acid changes^b	p.Arg752Cys; p.Val1089Met	p.Phe1072Thr; p.Ala1076Thr	p.Val908Leu	p.Val908Leu	p.Val908Leu	p.Thr851Met	p.Gln1695Ter*	p.Pro1677Leu*	p.(His1660ProfsTer5 2)*	p.(His1660ProfsTer5 2)*	p.Trp406GlyfsX135
Genomic coordinates^c	Chr2:74275298C>T; Chr2:74320791G>A	Chr2:74320741T>G; Chr2:74320752G>A	Chr2:74314999G>T	Chr2:74314999G>T	Chr2:74314999G>T	Chr2:74300733C>T	Chr2:74328998C>T	Chr2:74328945C>T	Chr2:74328892_74328898del	Chr2:74328892_74328898del	Chr2:74274259_74274259delA
CADD score	23.6; 29.1	28.2; 25.9	27	27	27	26.2	44	25.7	NA	NA	NA
gnomAD alleles	29 (0 homozygotes); 0	0; 0	0	0	0	0	0	0	0	0	0
Inheritance	AR	AR	AR	AR	AR	AD de novo	AD de novo	AD de novo	AD inherited	AD inherited	AD de novo
Ethnic origin	Caucasian	Caucasian	Asian	Asian	Asian	Caucasian	West Indies (father); Morocco (mother)	Estonian (mother); Finnish (father)	White British	White British	Ashkenazi Jewish
Sex	Female	Female	Male	Female	Female	Male	Male	Male	Male	Male	Male
Age at evaluation	7y 6m	3y 3m	21y	24y	27y	11m	7y 6m	18m	11y 0m	43y	9y 11m
Gestation	Term	41 weeks	Term	Term	Term	40 weeks	Term	35 weeks	Term	NA	40 weeks, 3 days
Growth											
Birth weight in g (SD)	3370 (-0.07)	3230 (-0.57)	1360 (-4.7)	NA	2270 (-2.44)	3865 (+0.66)	4300 (+1.49)	1475 (-2.37)	3170 (-0.73)	NA	3685 (+0.21)
Birth length in cm (SD)	48.3 (-0.92)	53.98 (+1.26)	NA	NA	NA	48.26 (-1.23)	53 (+0.68)	42 (-1.56)	NA	NA	57.2 (+2.38)
Birth OFC in cm (SD)	NA	NA	NA	NA	NA	35.56 (+0.52)	NA	31 (-0.66)	NA	NA	34.9 (+0.04)
Weight at evaluation in kg (SD)	41.7 (+2.42)	13.7 (-0.37)	38 (-5.16)	NA	47 (-1.52)	9.35 (-0.06)	27.7 (+0.79)	8.9 (-1.85; -3.0 Estonian chart)	38.55 (+0.36)	126 (>+2.0)	24.3 (-1.76)
Length/height at evaluation in cm (SD)	137.2 (+2.09)	100.3 (+1.13)	159 (-2.48)	NA	165 (+0.26)	75.5 (+0.41)	120 (-0.88)	82 (-0.10)	134.3 (-1.34)	185 (+1.15)	131 (-1.12)
OFC at evaluation in cm (SD)	56.5 (> +2.00)	47 (-1.04)	53 (-2.00)	NA	51 (< -2.00)	48.3 cm (+2.00)	55 (>+2.00)	50 (+1.98)	52.5 (-0.67)	56.5 (+0.67)	52 (-0.7)
Neurodevelopment											
Intellectual disability (degree)	Y (mild)	NA	Y (moderate)	Y (moderate)	Y (moderate)	NA	NA	NA	Y (moderate)	Y (mild to moderate)	N
Global developmental delay	Y	Y	Y	Y	Y	Y	Y	Y (severe)	Y	Y	Y
Gross motor delay	Y	Y	Y	Y	Y	Y	Y	Y	Y	NA	Y
Fine motor delay	Y	Y	Y	Y	Y	Y	Y	Y	Y	NA	N
Speech delay	Y	Y	Y	Y	Y	NA	NA	Y	Y	NA	Y
Behavior											
Autistic features/ASD	Y (obsessive-compulsive tendencies)	NA	NA	NA	NA	Y	NA	Y (poor eye contact)	Y (routine-oriented, obsessions)	N	Y
Difficult/delayed social interactions	Y	NA	NA	NA	NA	Y	NA	Y	Y	Y	Y
Other behavioral concerns	Anxiety, ADHD	High pain tolerance	NA	NA	NA	NA	NA	N	ADHD	Anxiety, depression	Anxiety, ADHD
Neurological Findings											
Seizures (type)	Y (? absence spells)	Y	N	N	N	N	Y (febrile partial and myoclonic)	Y (infantile spasms)	N	N	N

EEG	Abnormal focus on right	Abnormal	NA	NA	NA	Normal	Bioccipital bi-phasic spikes; then centro-temporal spikes with continuous spikes + waves during sleep	Epileptic activity	N	N	NA
Other abnormal movements	Tic disorder	Extensor posturing	N	N	N	Myoclonic movements and periodic limb movement in sleep	Dysmetria	Dystonias	N	N	N
Hypotonia	Y	Y	Y	Y	Y	Y	Y	Y (central)	N	N	N
Hypertonia	N	N	N	N	N	NA	N	Y (peripheral)	N	N	N
Brain MRI	Increased extra-axial spaces, mild ventriculomegaly	Normal	NA	NA	NA	Normal	Normal at 2.5y and 5.5y	Periventricular leukomalacia; increased extra-axial spaces	N	N	NA
Ophthalmological findings	No	Nystagmus	N	N	N	NA	N	Nystagmus; strabismus; ptosis; lacrimal duct stenosis	N	N	N
Cardiovascular anomalies	Cardiomegaly, valve abnormality, abnormal EKG	N	NA	NA	NA	NA	N	VSD, aortic valve insufficiency	N	N	N
Musculoskeletal findings	Advanced bone age; pes planus	Scoliosis	NA	NA	NA	N	N	Hip dysplasia	Joint hypermobility	NA	N
GI manifestations	Infantile feeding difficulties	Feeding difficulties/G-tube, constipation	NA	NA	NA	GER, delayed gastric emptying	NA	Feeding difficulties	N	N	N
Craniofacial dysmorphisms											
Brachycephaly	N	Y	NA	NA	NA	Y	N	N	Y	Y	N
Tall or broad forehead	Y	Y	Y	NA	Y	NA	Y	Y	N	N	N
Long face	Y	N	Y	NA	Y	NA	Y	Y	N	N	N
Protruding ears	N	Y	Y	NA	NA	NA	Y	Y	N	N	N
Short nose/long philtrum	Y	Y	N	NA	N	NA	N	Y	Y	N	N
Hypotonic face/open mouth	Y	Y	Y	NA	NA	NA	N	Y	N	N	N
Highly arched palate	Y	N	NA	NA	NA	Y	N	Y	N	N	N

^aAll cDNA variants based on NM_001287491.1. ^bAll amino acid changes based on NP_001274420.1. ^cGenomic coordinates based on GRCh37/hg19. *Denotes variants in last exon. Birth growth parameters plotted using Olsen *et al.* 2010 growth chart calculator; growth parameters for children 0-2 were plotted on WHO 0-2y growth charts; height and weight of older children/adults were plotted on CDC 2-20y growth charts; head circumferences/OFCs of children 2-5 plotted on 2-5 WHO growth charts and children/adults over 5 plotted on Nellhaus chart. If SD is significantly different on local growth chart, both are indicated. CADD, combined annotation dependent depletion; AR, autosomal recessive; AD, autosomal dominant; y, years; m, months; SD, standard deviation from the mean; OFC, occipitofrontal circumference (head circumference); Y, yes, indicates presence of feature; N, no, indicates absence of feature; NA, not available; ADHD, attention deficit hyperactivity disorder; VSD, ventricular septal defect; GER, gastroesophageal reflux; G-tube, gastrostomy tube.

Methods

Human subjects

Written informed consent was obtained from all individuals or family member legal representatives prior to exome sequencing. Individual 1 was counseled regarding the possible outcomes of exome sequencing and signed a consent form for research-based exome sequencing through the Baylor-Hopkins Center for Mendelian Genomics, which was approved by the Johns Hopkins Institutional Review Board (IRB). The rest of the participants were recruited through GeneMatcher²⁵. Individuals 2 and 4 were consented for clinical exome sequencing through Greenwood Genetic Center, and individual 8 was consented for clinical exome sequencing through GeneDx. Individuals 5 and 6 were consented for clinical and/or research-based exome sequencing. Individuals 3-I, 3-II, and 3-III were consented for research-based exome sequencing as described²², and individuals 7-I and 7-II were consented for research-based trio exome sequencing through the Deciphering Developmental Disorders (DDD) study³⁵.

Exome and Sanger sequencing

For individual 1, trio exome sequencing was performed on genomic DNA isolated from saliva through the Baylor-Hopkins Center for Mendelian Genomics at Johns Hopkins. Bi-allelic rare variants in *TET3* were identified using standard bioinformatics analysis. Sanger sequencing confirmed the presence of the *TET3* variants in the trio and their absence in an unaffected sibling. Individuals 2 and 4 had trio exome sequencing performed at Greenwood Genetic Center on a clinical basis. Standard bioinformatics analysis revealed bi-allelic (individual 2) and mono-allelic (individual 4) rare variants in *TET3*, which were subsequently confirmed by Sanger sequencing. Individuals 3-I, 3-II, and 3-III had exome sequencing performed as described²². Individual 5 had trio exome sequencing performed with standard bioinformatics analysis, which identified a *de novo* monoallelic variant in *TET3*; the variant was confirmed with Sanger sequencing. Individual 6 had clinical trio exome sequencing performed, which did not reveal pathogenic mutations in genes known to be associated with Mendelian disorders. Reanalysis at the Broad Institute of MIT and Harvard identified a rare *de novo* *TET3* missense variant, which was subsequently confirmed with Sanger sequencing. Individual 7 had trio exome sequencing performed as part of the DDD study³⁵; the rare inherited mono-allelic variant in *TET3* was identified in the proband and his similarly-affected father using standard bioinformatics analysis. Sanger sequencing confirmed the presence of the *TET3* variant in the affected proband and his father and its absence in the mother

and an unaffected sibling. Individual 8 had trio exome sequencing performed on a clinical basis through GeneDx. Standard bioinformatics analysis was performed and revealed a *de novo* mono-allelic variant in *TET3*, which was confirmed by Sanger sequencing. All patients reported have no known definitive pathogenic variants identified in genes causative for developmental delay.

Cells

HEK 293 cells were cultured in Dulbecco's modified Eagle's medium (DMEM; Gibco) containing 10% fetal bovine serum (FBS; Sigma), 2 mM L-Glutamine (Gibco), MEM Non-essential amino acid solution (Sigma), sodium pyruvate (Sigma), and Penicillin Streptomycin.

Cloning and plasmids

Full-length human *TET3* coding sequence was amplified from cDNA and cloned into the pINTO-N3 plasmid backbone. The pINTO-N3 vector was based on the pINTO system³⁶, containing three N-terminal epitope tags (FLAG, HA, and Twin-Strep-Tag). Point mutations were introduced into the *hTET3* coding sequence via Gibson assembly and verified by Sanger sequencing.

5hmC dot blot

HEK 293 cells were transiently transfected with plasmids using Lipofectamine 3000 (Thermo Fisher). Cells were harvested 48 hours post transfection, lysed in Proteinase K buffer (100 mM NaCl, 10 mM Tris-HCl pH 8.0, 10mM EDTA, 0.5% SDS), and sonicated for 20 minutes (30 seconds ON, 30 seconds OFF) using a Bioruptor (Diagenode, NJ). A portion of the cell lysate was used to perform a Western blot with an HA antibody (#901501 BioLegend, CA) to verify hTET3 protein expression. The remaining cell lysate was incubated with Proteinase K (Ambion AM2548) for 45 minutes at 50°C and DNA was extracted using Phenol-Chloroform Isoamyl Alcohol (PCIA). DNA was denatured for 10 minutes at 95°C in 100 mM NaOH and 10 mM EDTA and then neutralized by addition of 2M ammonium acetate (pH 7.0). Denatured DNA was transferred to a BrightStar-Plus Nylon membrane (Ambion AM10102) using a Bio-Dot microfiltration apparatus (Bio-Rad) according to the manufacturer's instructions. Briefly, the membrane was rinsed in 6X SSC buffer before assembling the apparatus and the DNA samples were loaded onto the membrane under vacuum pressure. The membrane was rinsed in 2X SSC and then dried for 15 minutes at 80°C in a hybridization oven. The membrane was then crosslinked twice with 200 mJ/cm² UVA (254 nm) using a Spectrolinker (Spectroline, NY). Next, the membrane was stained

with a 0.04% solution of Methylene Blue (Sigma 66720) to visualize total DNA. A Western blot was then performed to detect 5hmC using a 5hmC antibody (Active Motif 39770).

Dot blot quantification and analysis

Dot blot quantification was performed using ImageJ as described in the ImageJ documentation. Raw TIFF files were opened in ImageJ and the “Integrated Density” measurement of each dot was recorded after correcting for background. To account for potential differences in total DNA amount across samples, the 5hmC signal was divided by the Methylene Blue signal for each dot. The normalized 5hmC signal was averaged across biological replicates and divided by the normalized 5hmC signal in the wild-type *hTET3* transfection to obtain a relative 5hmC signal. Samples in which the transfected mutant *hTET3* was expressed at lower levels than the wild-type control were not further considered in the analysis. These were the only data points excluded from the final quantification.

Mutation Modeling

Mutations in *TET3* were mapped onto the well-conserved TET2 catalytic domain crystal structure (PDB accession 5DEU ²⁶) using UCSF Chimera ³⁷.

References

1. Fahrner, J.A., and Bjornsson, H.T. (2014). Mendelian disorders of the epigenetic machinery: tipping the balance of chromatin states. *Annu Rev Genomics Hum Genet* 15, 269-293.
2. Larizza, L., and Finelli, P. (2019). Developmental disorders with intellectual disability driven by chromatin dysregulation: Clinical overlaps and molecular mechanisms. *Clin Genet* 95, 231-240.
3. Tatton-Brown, K., Seal, S., Ruark, E., Harmer, J., Ramsay, E., Del Vecchio Duarte, S., Zachariou, A., Hanks, S., O'Brien, E., Aksglaede, L., et al. (2014). Mutations in the DNA methyltransferase gene DNMT3A cause an overgrowth syndrome with intellectual disability. *Nat Genet* 46, 385-388.
4. Ehrlich, M., Buchanan, K.L., Tsien, F., Jiang, G., Sun, B., Uicker, W., Weemaes, C.M., Smeets, D., Sperling, K., Belohradsky, B.H., et al. (2001). DNA methyltransferase 3B mutations linked to the ICF syndrome cause dysregulation of lymphogenesis genes. *Hum Mol Genet* 10, 2917-2931.
5. Mnatzakanian, G.N., Lohi, H., Munteanu, I., Alfred, S.E., Yamada, T., MacLeod, P.J., Jones, J.R., Scherer, S.W., Schanen, N.C., Friez, M.J., et al. (2004). A previously unidentified MECP2 open reading frame defines a new protein isoform relevant to Rett syndrome. *Nat Genet* 36, 339-341.
6. Tahiliani, M., Koh, K.P., Shen, Y., Pastor, W.A., Bandukwala, H., Brudno, Y., Agarwal, S., Iyer, L.M., Liu, D.R., Aravind, L., et al. (2009). Conversion of 5-methylcytosine to 5-hydroxymethylcytosine in mammalian DNA by MLL partner TET1. *Science* 324, 930-935.
7. Ito, S., D'Alessio, A.C., Taranova, O.V., Hong, K., Sowers, L.C., and Zhang, Y. (2010). Role of Tet proteins in 5mC to 5hmC conversion, ES-cell self-renewal and inner cell mass specification. *Nature* 466, 1129-1133.
8. Wu, X., and Zhang, Y. (2017). TET-mediated active DNA demethylation: mechanism, function and beyond. *Nat Rev Genet* 18, 517-534.
9. Ito, S., Shen, L., Dai, Q., Wu, S.C., Collins, L.B., Swenberg, J.A., He, C., and Zhang, Y. (2011). Tet proteins can convert 5-methylcytosine to 5-formylcytosine and 5-carboxylcytosine. *Science* 333, 1300-1303.
10. He, Y.F., Li, B.Z., Li, Z., Liu, P., Wang, Y., Tang, Q., Ding, J., Jia, Y., Chen, Z., Li, L., et al. (2011). Tet-mediated formation of 5-carboxylcytosine and its excision by TDG in mammalian DNA. *Science* 333, 1303-1307.
11. Globisch, D., Munzel, M., Muller, M., Michalakis, S., Wagner, M., Koch, S., Bruckl, T., Biel, M., and Carell, T. (2010). Tissue distribution of 5-hydroxymethylcytosine and search for active demethylation intermediates. *PLoS One* 5, e15367.
12. Mayer, W., Niveleau, A., Walter, J., Fundele, R., and Haaf, T. (2000). Demethylation of the zygotic paternal genome. *Nature* 403, 501-502.
13. Wossidlo, M., Nakamura, T., Lepikhov, K., Marques, C.J., Zakhartchenko, V., Boiani, M., Arand, J., Nakano, T., Reik, W., and Walter, J. (2011). 5-Hydroxymethylcytosine in the mammalian zygote is linked with epigenetic reprogramming. *Nat Commun* 2, 241.
14. Iqbal, K., Jin, S.G., Pfeifer, G.P., and Szabo, P.E. (2011). Reprogramming of the paternal genome upon fertilization involves genome-wide oxidation of 5-methylcytosine. *Proc Natl Acad Sci U S A* 108, 3642-3647.

15. Inoue, A., Shen, L., Dai, Q., He, C., and Zhang, Y. (2011). Generation and replication-dependent dilution of 5fC and 5caC during mouse preimplantation development. *Cell Res* 21, 1670-1676.
16. Inoue, A., Matoba, S., and Zhang, Y. (2012). Transcriptional activation of transposable elements in mouse zygotes is independent of Tet3-mediated 5-methylcytosine oxidation. *Cell Res* 22, 1640-1649.
17. Gu, T.P., Guo, F., Yang, H., Wu, H.P., Xu, G.F., Liu, W., Xie, Z.G., Shi, L., He, X., Jin, S.G., et al. (2011). The role of Tet3 DNA dioxygenase in epigenetic reprogramming by oocytes. *Nature* 477, 606-610.
18. Zhu, X., Girardo, D., Govek, E.E., John, K., Mellen, M., Tamayo, P., Mesirov, J.P., and Hatten, M.E. (2016). Role of Tet1/3 Genes and Chromatin Remodeling Genes in Cerebellar Circuit Formation. *Neuron* 89, 100-112.
19. Yu, H., Su, Y., Shin, J., Zhong, C., Guo, J.U., Weng, Y.L., Gao, F., Geschwind, D.H., Coppola, G., Ming, G.L., et al. (2015). Tet3 regulates synaptic transmission and homeostatic plasticity via DNA oxidation and repair. *Nat Neurosci* 18, 836-843.
20. Li, X., Wei, W., Zhao, Q.Y., Widagdo, J., Baker-Andresen, D., Flavell, C.R., D'Alessio, A., Zhang, Y., and Bredy, T.W. (2014). Neocortical Tet3-mediated accumulation of 5-hydroxymethylcytosine promotes rapid behavioral adaptation. *Proc Natl Acad Sci U S A* 111, 7120-7125.
21. Lek, M., Karczewski, K.J., Minikel, E.V., Samocha, K.E., Banks, E., Fennell, T., O'Donnell-Luria, A.H., Ware, J.S., Hill, A.J., Cummings, B.B., et al. (2016). Analysis of protein-coding genetic variation in 60,706 humans. *Nature* 536, 285-291.
22. Santos-Cortez, R.L.P., Khan, V., Khan, F.S., Mughal, Z.U., Chakchouk, I., Lee, K., Rasheed, M., Hamza, R., Acharya, A., Ullah, E., et al. (2018). Novel candidate genes and variants underlying autosomal recessive neurodevelopmental disorders with intellectual disability. *Hum Genet* 137, 735-752.
23. Tatton-Brown, K., Loveday, C., Yost, S., Clarke, M., Ramsay, E., Zachariou, A., Elliott, A., Wylie, H., Ardisson, A., Rittinger, O., et al. (2017). Mutations in Epigenetic Regulation Genes Are a Major Cause of Overgrowth with Intellectual Disability. *Am J Hum Genet* 100, 725-736.
24. Bjornsson, H.T. (2015). The Mendelian disorders of the epigenetic machinery. *Genome Res* 25, 1473-1481.
25. Sobreira, N., Schiettecatte, F., Boehm, C., Valle, D., and Hamosh, A. (2015). New tools for Mendelian disease gene identification: PhenoDB variant analysis module; and GeneMatcher, a web-based tool for linking investigators with an interest in the same gene. *Hum Mutat* 36, 425-431.
26. Hu, L., Lu, J., Cheng, J., Rao, Q., Li, Z., Hou, H., Lou, Z., Zhang, L., Li, W., Gong, W., et al. (2015). Structural insight into substrate preference for TET-mediated oxidation. *Nature* 527, 118-122.
27. Boukas, L., Havrilla, J.M., Hickey, P.F., Quinlan, A.R., Bjornsson, H.T., and Hansen, K.D. (2019). Coexpression patterns define epigenetic regulators associated with neurological dysfunction. *Genome Res* 29, 532-542.
28. Faundes, V., Newman, W.G., Bernardini, L., Canham, N., Clayton-Smith, J., Dallapiccola, B., Davies, S.J., Demos, M.K., Goldman, A., Gill, H., et al. (2018). Histone Lysine Methylases

- and Demethylases in the Landscape of Human Developmental Disorders. *Am J Hum Genet* 102, 175-187.
29. Martin, H.C., Jones, W.D., McIntyre, R., Sanchez-Andrade, G., Sanderson, M., Stephenson, J.D., Jones, C.P., Handsaker, J., Gallone, G., Bruntraeger, M., et al. (2018). Quantifying the contribution of recessive coding variation to developmental disorders. *Science* 362, 1161-1164.
 30. Rainger, J., Pehlivan, D., Johansson, S., Bengani, H., Sanchez-Pulido, L., Williamson, K.A., Ture, M., Barker, H., Rosendahl, K., Spranger, J., et al. (2014). Monoallelic and biallelic mutations in MAB21L2 cause a spectrum of major eye malformations. *Am J Hum Genet* 94, 915-923.
 31. Chong, J.X., McMillin, M.J., Shively, K.M., Beck, A.E., Marvin, C.T., Armenteros, J.R., Buckingham, K.J., Nkinsi, N.T., Boyle, E.A., Berry, M.N., et al. (2015). De novo mutations in NALCN cause a syndrome characterized by congenital contractures of the limbs and face, hypotonia, and developmental delay. *Am J Hum Genet* 96, 462-473.
 32. Perera, A., Eisen, D., Wagner, M., Laube, S.K., Kunzel, A.F., Koch, S., Steinbacher, J., Schulze, E., Splith, V., Mittermeier, N., et al. (2015). TET3 is recruited by REST for context-specific hydroxymethylation and induction of gene expression. *Cell Rep* 11, 283-294.
 33. Luscan, A., Laurendeau, I., Malan, V., Francannet, C., Odent, S., Giuliano, F., Lacombe, D., Touraine, R., Vidaud, M., Pasmant, E., et al. (2014). Mutations in SETD2 cause a novel overgrowth condition. *J Med Genet* 51, 512-517.
 34. Imagawa, E., Higashimoto, K., Sakai, Y., Numakura, C., Okamoto, N., Matsunaga, S., Ryo, A., Sato, Y., Sanefuji, M., Ihara, K., et al. (2017). Mutations in genes encoding polycomb repressive complex 2 subunits cause Weaver syndrome. *Hum Mutat* 38, 637-648.
 35. Deciphering Developmental Disorders, S. (2017). Prevalence and architecture of de novo mutations in developmental disorders. *Nature* 542, 433-438.
 36. Gao, Z., Zhang, J., Bonasio, R., Strino, F., Sawai, A., Parisi, F., Kluger, Y., and Reinberg, D. (2012). PCGF homologs, CBX proteins, and RYBP define functionally distinct PRC1 family complexes. *Mol Cell* 45, 344-356.
 37. Pettersen, E.F., Goddard, T.D., Huang, C.C., Couch, G.S., Greenblatt, D.M., Meng, E.C., and Ferrin, T.E. (2004). UCSF Chimera--a visualization system for exploratory research and analysis. *J Comput Chem* 25, 1605-1612.

Web Resources:

CADD, <http://cadd.gs.washington.edu/>

ClinVar, <https://www.ncbi.nlm.nih.gov/clinvar/>

gnomAD Browser, <http://gnomad.broadinstitute.org/>

OMIM, <http://www.omim.org/>

PyMOL, <https://pymol.org/2>

RCSB Protein Data Bank, <http://www.rcsb.org/pdb/home/home.do>

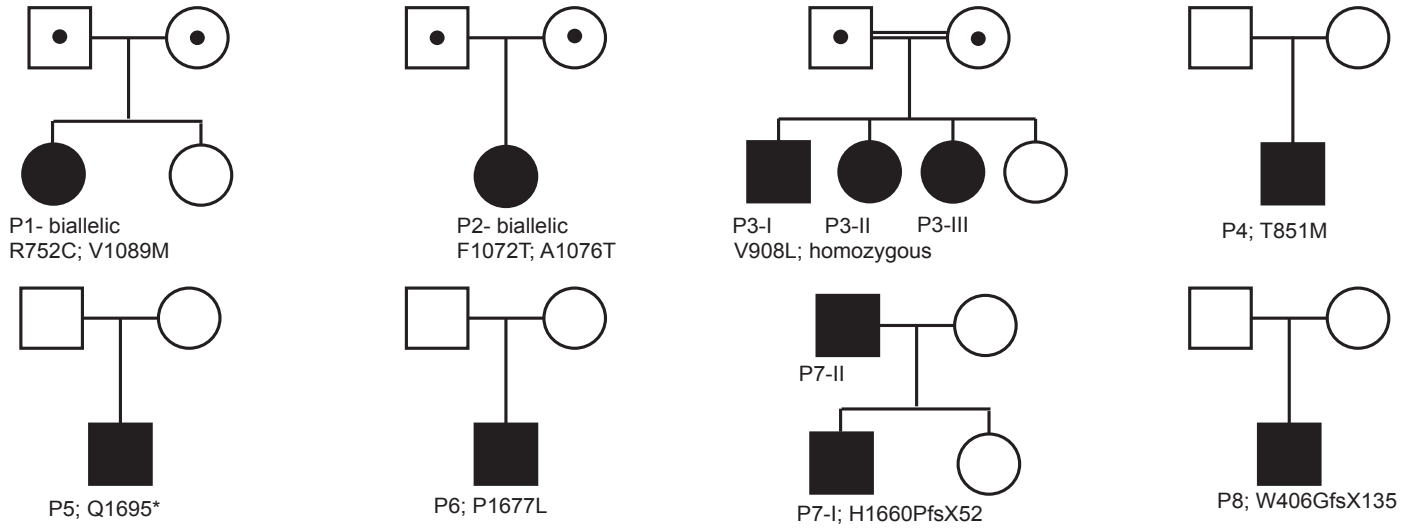


Figure 1. Inheritance patterns and variants in individuals with *TET3* deficiency. Pedigrees illustrating inheritance patterns in each family with specific variants listed.

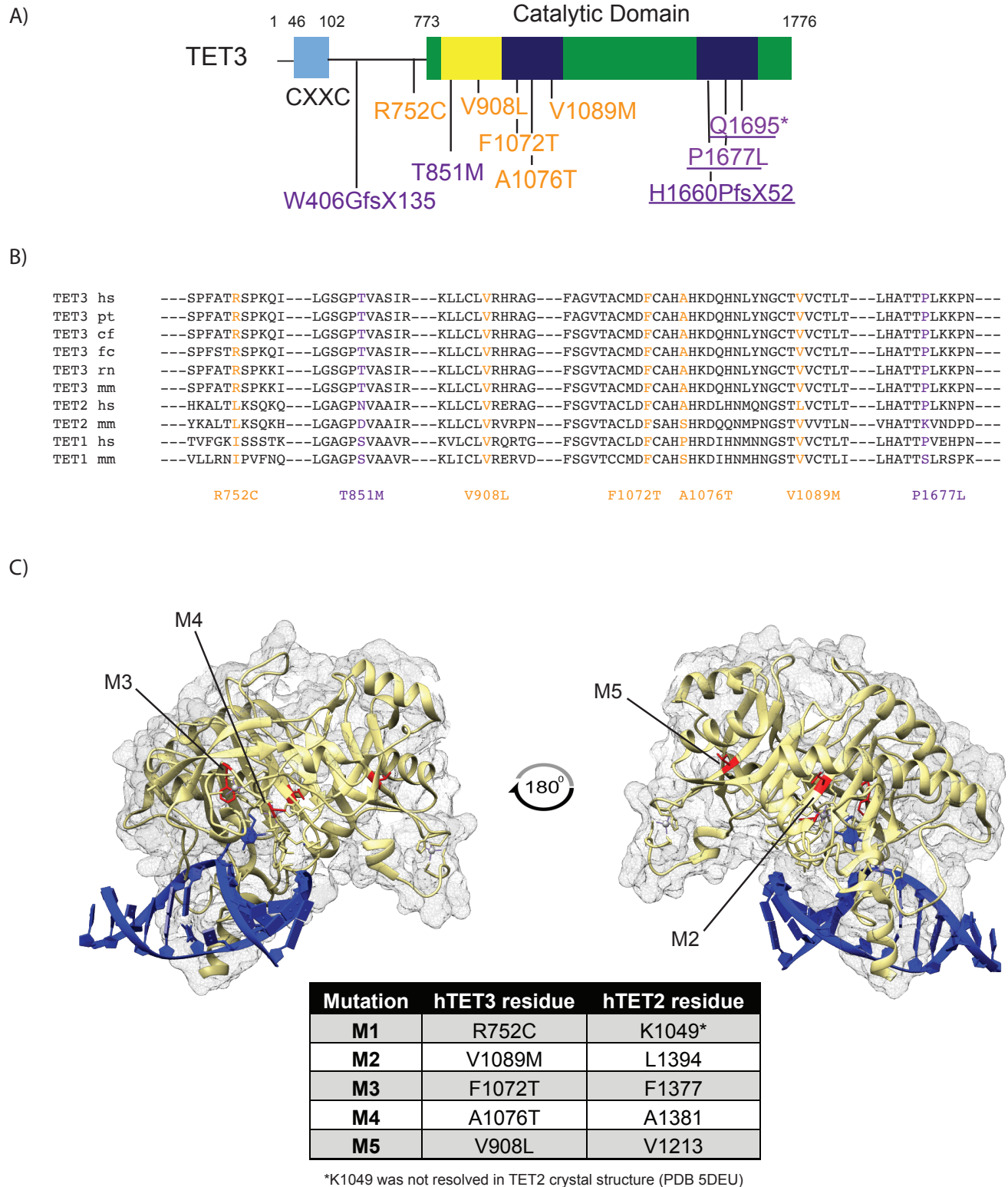


Figure 2. TET3 variants and predicted functional consequences. (A) Schematic of TET3 protein showing domain structure with the catalytic dioxxygenase domain in green (aa, amino

acids 773-1776) and specific subdomains indicated as follows: the Cys-rich insert in yellow (aa 825-1012) and the double-stranded β helix domain in dark blue (DSBH; aa 1012-1159; aa 1636-1719). The DSBH domain is separated by a low complexity insert. The N-terminal CXXC DNA binding domain is shown in light blue (aa 46-102). Specific variants are annotated in orange for recessive alleles and purple for dominant alleles, and underlined variants occur within the last exon. **(B)** Alignment of missense variants in *TET3* across multiple species, including hs, *Homo sapiens*; pt, *Pan troglodytes*; cf, *Canis familiaris*; fc, *Felis catus*; rn, *Rattus norvegicus*; and mm, *Mus musculus*, and among TET enzymes. **(C)** Crystal structure of TET2 bound to DNA with highlighted *TET3* mutations M2, M3, M4, and M5.

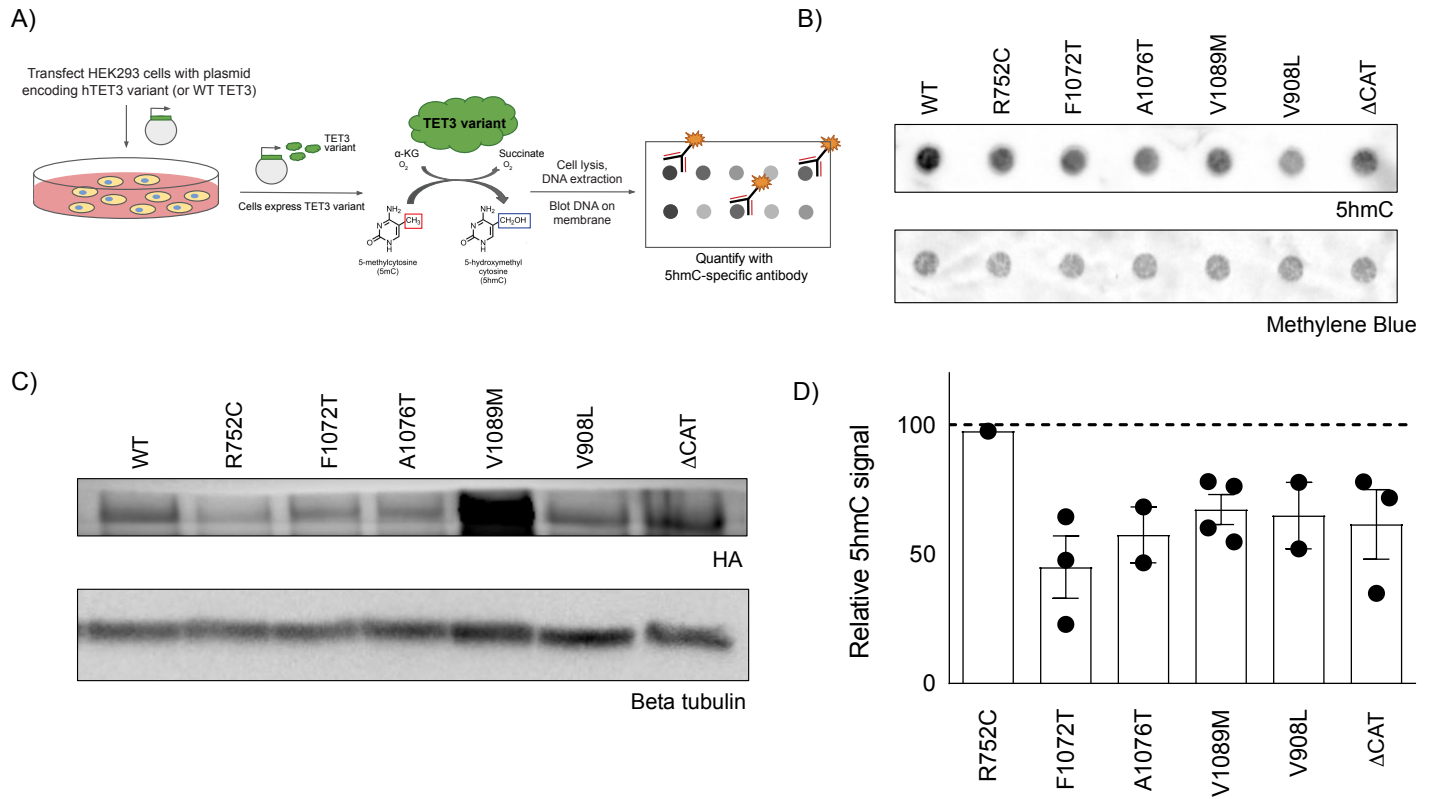


Figure 3. Cells overexpressing *TET3* variants have decreased levels of 5hmC. (A) Schematic outlining enzymatic activity assay for measuring TET3 catalytic activity. (B) Representative dot blot showing 5hmC levels in HEK293 cells overexpressing wild-type or mutant HA-tagged *TET3* constructs. (C) Representative Western blot showing wild-type and mutant TET3 protein expression in HEK293 cells. Tubulin was used as loading control. (D) Quantification of 5hmC signal relative to wild type. The dotted line indicates wild type signal. Error bars represent standard error of the mean. WT, wild type; Δ cat, catalytically inactive control.